Bi-Objective Electric Vehicle Charging Scheduling Under Stochastic Charging Durations

Aimen Khiar [a,b], Mohamed El Amine Brahmia [b], Mahmoud Golabi [a], Abdennour Azerine [a], and Lhassane Idoumghar [a]

[a]IRIMAS UR 7499, University of Haute Alsace, Mulhouse, France
Email: {aimen.khiar, mahmoud.golabi, abdennour.azerine, lhassane.idoumghar}@uha.fr
[b]CESI LINEACT UR 7527, Strasbourg, France
Email: {akhiar, abrahmia}@cesi.fr

***Abstract*—This paper addresses the electric vehicle charging scheduling problem under stochastic charging durations, where uncertainty arises from variations in actual charging times that are typically assumed deterministic in existing literature. We formulate a bi-objective optimization problem minimizing the expected values of peak load and total tardiness. We explicitly enforce non-overlapping charging sessions within the objective function evaluation via a repair mechanism where this latter induces cascading stochastic dependencies. This makes both realized charging start and end times random variables, substantially increasing problem complexity compared to existing approaches. We derive the cumulative distribution functions of realized charging start and end times and obtain an analytical expression for expected total tardiness involving a high-dimensional integral, while showing that expected peak load is intractable to compute exactly. We therefore approximate both objectives using Monte Carlo simulation. To solve the problem, we adapt and compare three multi-objective evolutionary algorithms: NSGA-II, MOPSO, and MOGWO. Comprehensive computational experiments on 20 real-world instances derived from the ACN-Data dataset, involving up to 200 vehicles, show that NSGA-II achieves superior hypervolume performance on 15 out of 20 instances, with statistically significant differences confirmed by Friedman and Mann–Whitney U tests. The proposed framework provides an effective decision-support approach for managing electric vehicle charging operations under uncertainty.**

***Index Terms*—Stochastic optimization; electric vehicle charging scheduling; multi-objective optimization; evolutionary algorithms**

I. Introduction

The electric vehicle (EV) market has experienced exponential growth in recent years, with global sales surging from approximately 0.3 million units in 2014 to over 17 million units in 2024, driven by several factors such as environmental concerns and rapid battery technology advancements [1]. This expansion, combined with the relatively long charging times of EVs that often extend to several hours [2], [3], has created critical challenges for charging infrastructure, necessitating designing intelligent scheduling systems capable of efficiently managing large-scale operations while minimizing grid stress and service delays, giving rise to the EV charging scheduling problem (EVCSP).

Real-world EV charging operations are subject to inherent variability in charging durations due to factors largely beyond the operator's control, such as the initial battery state of charge, fluctuations in grid demand, simultaneous usage of charging stations, and ambient temperature conditions. Moreover, the energy requested upon arrival may differ from the amount communicated in advance. Incorporating these sources of stochasticity into scheduling models is therefore essential to accurately represent operational conditions and to develop solution approaches that remain robust in dynamic and uncertain environments [3].

Motivated by the fact that most of the existing literature treats charging durations as deterministic [4], [5], we develop a scheduling framework for EV charging operations under stochastic charging times. The resulting bi-criteria formulation seeks to minimize the expected peak load and the expected total tardiness. Given the problem's NP-hardness [3], we adapt and compare three well-established multi-objective evolutionary algorithms (MOEAs): NSGA-II, MOPSO, and MOGWO. Through comprehensive computational experiments and statistical validation, we identify the best-performing algorithm for this stochastic optimization setting. To the best of our knowledge, this work is among the very few studies in the EVCSP literature that explicitly account for stochastic charging durations, following the pioneering work of Khiar et al. [3].

The remainder of this paper is organized as follows. Section II reviews related literature on deterministic and stochastic approaches to EVCSP. Section III formulates the stochastic scheduling problem. Section IV derives probability distributions for realized charging times and an analytical expression for expected tardiness. Section V presents the proposed solution approach. Section VI reports computational experiments and statistical comparisons. Section VII concludes the paper and identifies future research directions.

II. Related Works

Research on EVCSP can be broadly categorized into deterministic and stochastic approaches, each addressing different aspects of the inherent complexities in EV charging management.

A. Deterministic Approaches

In the deterministic domain, several recent works have made significant contributions to solving the EVCSP under various operational constraints. Azerine et al. [6] developed a hybrid memetic algorithm that integrates evolutionary optimization with mathematical programming to address the multi-station EVCSP. Their approach maximizes satisfied charging demands while managing heterogeneous chargers and limited grid capacities across multiple charging stations. Complementing this work, Golabi et al. [4] proposed a hybrid optimization framework combining genetic algorithms with mathematical programming and a multi-surrogate-assisted strategy to efficiently tackle large-scale NP-hard instances at public charging stations, with the objective of minimizing deviations from user-requested state-of-charge levels under grid and charger constraints.

From a multi-objective optimization perspective, Khiar et al. [7] developed a framework that simultaneously minimizes peak energy consumption while maximizing user satisfaction through metaheuristic algorithms. Similarly, Zaidi et al. [8] formulated a mixed-integer linear programming (MILP) model to minimize both peak grid power and charger deployment costs, employing hybrid iterated local search method for optimal solution approximation.

B. Stochastic Approaches

While deterministic methods provide valuable insights, real-world charging operations are inherently subject to uncertainties in charging durations, arrival patterns, and energy demand [9]–[11]. To address these stochastic elements, several researchers have developed probabilistic frameworks. Gao et al. [12] proposed a two-stage stochastic programming model for integrated energy scheduling under uncertain container loads, while Emami et al. [10] developed a stochastic MILP model for bus electrification, leveraging Benders decomposition to handle random charging demand effectively. Wang et al. [13] presented a scenario-based two-stage stochastic model for real-time scheduling that addresses uncertain EV availability and electricity demand through a rolling window approach. More recently, James et al. [14] introduced a stochastic EV charging framework that models uncertain charging patterns via Monte Carlo simulation coupled with backward–forward sweep load flow analysis to evaluate the aggregated impact on grid stability, demonstrating the superiority of coordinated charging strategies over deterministic alternatives.

C. Research Gap and Contribution

Despite these significant advances in stochastic modeling, most existing approaches assume that charging durations become deterministic once charging sessions commence, thereby overlooking the substantial variations in actual charging times that can significantly impact schedule quality and operational performance.

To the best of our knowledge, Khiar et al. [3] provided the only study that explicitly considered the EVCSP under stochastic charging durations. They formulated a multi-objective optimization problem that minimizes the conditional expected values of peak load, total tardiness, and total undelivered energy. Their work established that this problem is strongly NP-hard under uncertainty and employed MOEAs to approximate the Pareto front. In their formulation, objective functions are defined as conditional expectations and computed with respect to probabilistic events that ensure non-overlapping charging sessions on each charger.

Building on this foundation, we tackle the EVCSP with stochastic charging durations from a different perspective by explicitly enforcing non-overlapping charging sessions during the evaluation of objective function rather than relying on probabilistic conditioning, thereby distinguishing our approach from existing work. Specifically, when actual charging durations are realized during schedule execution, temporal conflicts between consecutive sessions are resolved through a repair mechanism: if two sessions overlap on the same charger, the subsequent vehicle waits until the preceding vehicle completes charging. This introduces a fundamental difference in the stochastic structure of the problem.

Whereas the formulation in [3] implies that only charging end times are random variables, our formulation—through the repair mechanism—treats both start and end times as random variables. This distinction arises because each vehicle's actual start time depends on the realized end times of all preceding vehicles assigned to the same charger, thereby inducing a cascading dependency structure throughout the schedule.

III. Scheduling Model

We consider a continuous-time scheduling horizon $\mathcal{H} \subseteq \mathbb{R}_{>0}$ with $\mathbb{R}_{>0} = \{x \in \mathbb{R} \mid x > 0\}$. An instance of the EVCSP is characterized by n charging requests indexed by $[n] = \{1, \ldots, n\}$. Each request $i \in [n]$ is specified by the triple $(a_i, d_i, e_i) \in \mathbb{R}^3_{>0}$, where a_i denotes the arrival time, d_i denotes the departure time requested by the client with $a_i < d_i$, and e_i denotes the energy requirement measured in kilowatt-hours (kWh).

The charging infrastructure consists of m chargers indexed by $[m] = \{1, \ldots, m\}$, where charger $j \in [m]$ delivers constant power output w_j (measured in kilowatts, kW). We assume that each EV remains connected to its assigned charger from the commencement of charging until completion. Let $m^{(d)} \in \mathbb{R}_{>0}$ denote the minimum delay between consecutive charging sessions on the same charger, representing the changeover time required to switch connections between EVs.

For each vehicle-charger pair $(i, j) \in [n] \times [m]$, let $\tau_{i,j}$ denote the random charging duration having a probability distribution with positive support. For tractability, we assume that the random variables $\{\tau_{i,j}\}_{i \in [n], j \in [m]}$ are mutually independent (see [3]).

Definition 1 (Feasible Schedule): A feasible schedule S for the present EVCSP consists of:

1) A charger assignment function $\sigma : [n] \to [m]$, where $\sigma(i)$ specifies the charger assigned to EV i;
2) Planned charging start times $t_i^{(s)} \in \mathcal{H}$ for each $i \in [n]$, satisfying $t_i^{(s)} \geq a_i$, representing the scheduled posi-

tioning of charging sessions prior to the realization of random durations.

To characterize the sequencing of EVs on each charger, we introduce adjacency mappings.

Definition 2 (Predecessor-Successor Mappings): Define functions $pred, succ : [n] \to [n] \cup \{0\}$ such that for any $i_1, i_2 \in [n]$:

- $succ(i_1) = i_2$ if and only if $\sigma(i_1) = \sigma(i_2)$ and EV i_2 immediately follows EV i_1 in the charging sequence on charger $\sigma(i_1)$ according to the planned start times $\{t_i^{(s)}\}_{i\in[n]}$. Moreover, $succ(i_1) = 0$ if EV i_1 is the last EV scheduled on charger $\sigma(i_1)$.
- $pred(i_1) = i_2$ if and only if $\sigma(i_1) = \sigma(i_2)$ and EV i_2 immediately precedes EV i_1 in the charging sequence on charger $\sigma(i_1)$ according to the planned start times. Moreover, $pred(i_1) = 0$ if EV i_1 is the first EV scheduled on charger $\sigma(i_1)$.

The realized charging start time $\widetilde{t}_i^{(s)}$ for EV $i \in [n]$ is determined by the scheduled time $t_i^{(s)}$ and the completion time of its immediate predecessor, if any. Formally,

$$\widetilde{t}_i^{(s)} = \begin{cases} t_i^{(s)}, & \text{if } pred(i) = 0, \\ \max\left(t_i^{(s)}, \widetilde{t}_{pred(i)}^{(e)} + m^{(d)}\right), & \text{otherwise,} \end{cases} \quad (1)$$

where $\mathbb{I}\{\cdot\}$ denotes the indicator function. The realized charging end time is given by

$$\widetilde{t}_i^{(e)} = \widetilde{t}_i^{(s)} + \tau_{i,\sigma(i)}. \quad (2)$$

We now define the random quantities $\mathbf{P}$ and $\mathbf{T}$ representing the peak load and total tardiness, respectively, given by

$$\mathbf{P} = \max_{t\in\mathcal{H}} \sum_{i\in[n]} w_{\sigma(i)} \mathbb{I}\left\{\widetilde{t}_i^{(s)} \le t \le \widetilde{t}_i^{(e)}\right\}, \quad (3)$$

and

$$\mathbf{T} = \sum_{i\in[n]} \max\left(0, \widetilde{t}_i^{(e)} - d_i\right), \quad (4)$$

where $\mathbf{P}$ captures the maximum instantaneous power demand across the scheduling horizon, and $\mathbf{T}$ measures the total delay with respect to requested departure times.

The bi-objective optimization problem seeks to determine a charger assignment σ and planned start times $\{t_i^{(s)}\}_{i\in[n]}$ that minimize the expected values

$$f_1 = \mathbb{E}(\mathbf{P}), \quad \text{and} \quad f_2 = \mathbb{E}(\mathbf{T}). \quad (5)$$

IV. Theoretical Analysis

In this section, we characterize the probability distributions of the realized charging times $\widetilde{t}_i^{(s)}$ and $\widetilde{t}_i^{(e)}$ induced by stochastic charging durations, and derive an explicit formula for the expected total tardiness $f_2 = \mathbb{E}(\mathbf{T})$.

To simplify notation, we define the auxiliary function

$$\alpha_\ell(z, \mathbf{y}) := z - \ell \cdot m^{(d)} - \sum_{j=1}^{\ell} y_{k-j+1}, \quad (6)$$

where $\mathbf{y} = (y_k, y_{k-1}, \ldots, y_{k-\ell+1}) \in \mathbb{R}^\ell_{>0}$ and $1 \le \ell \le l$. Moreover, we denote by f_i the probability density function of the charging duration $\tau_{i,\sigma(i)}$ for EV i at its assigned charger $\sigma(i)$, and by $F_i^{(s)}$ and $F_i^{(e)}$ the cumulative distribution functions of the realized charging start and end times $\widetilde{t}_i^{(s)}$ and $\widetilde{t}_i^{(e)}$, respectively.

Proposition 1: For any EV $i \in [n]$ and $z \in \mathbb{R}_{>0}$, the cumulative distribution function of the realized charging start time can be computed recursively by the formula:

$$F_i^{(s)}(z) = \begin{cases} \mathbb{I}\{t_i^{(s)} \le z\}, & \text{if } pred(i) = 0, \\ \mathbb{I}\{t_i^{(s)} \le z\} \cdot \mathcal{I}_i(z), & \text{otherwise,} \end{cases} \quad (7)$$

where $\mathcal{I}_i(z)$ is defined as:

$$\mathcal{I}_i(z) = \int_0^\infty F_{pred(i)}^{(s)}(z - m^{(d)} - y) f_{pred(i)}(y)\, dy. \quad (8)$$

Proof. We proceed by considering the two cases determined by the predecessor function.

Case 1: $pred(i) = 0$**.** When EV i is the first EV scheduled on charger $\sigma(i)$, we have $\widetilde{t}_i^{(s)} = t_i^{(s)}$ by definition. Since $t_i^{(s)}$ is a deterministic planned start time, the event $\{\widetilde{t}_i^{(s)} \le z\}$ is equivalent to $\{t_i^{(s)} \le z\}$, yielding

$$F_i^{(s)}(z) = \mathbb{I}\{t_i^{(s)} \le z\}.$$

Case 2: $pred(i) = i'$ **for some** $i' \in [n] \setminus \{i\}$. When EV i has an immediate predecessor i', we have

$$\widetilde{t}_i^{(s)} = \max\left(t_i^{(s)}, \widetilde{t}_{i'}^{(e)} + m^{(d)}\right).$$

For the maximum of two quantities to be at most z, both quantities must be at most z. Therefore,

$$\begin{aligned} F_i^{(s)}(z) &= \mathbb{P}\left(t_i^{(s)} \le z \text{ and } \widetilde{t}_{i'}^{(e)} + m^{(d)} \le z\right) \\ &= \mathbb{P}\left(t_i^{(s)} \le z\right) \cdot \mathbb{P}\left(\widetilde{t}_{i'}^{(e)} \le z - m^{(d)}\right), \end{aligned}$$

where the factorization holds because $t_i^{(s)}$ is deterministic and $\widetilde{t}_{i'}^{(e)}$ depends only on random charging durations. Since $t_i^{(s)}$ is deterministic, $\mathbb{P}(t_i^{(s)} \le z) = \mathbb{I}\{t_i^{(s)} \le z\}$.

Recall that $\widetilde{t}_{i'}^{(e)} = \widetilde{t}_{i'}^{(s)} + \tau_{i',\sigma(i')}$. Using the law of total probability and conditioning on $\tau_{i',\sigma(i')} = y$, we obtain

$$\begin{aligned} \mathbb{P}\left(\widetilde{t}_{i'}^{(e)} \le z - m^{(d)}\right) &= \mathbb{P}\left(\widetilde{t}_{i'}^{(s)} + \tau_{i',\sigma(i')} \le z - m^{(d)}\right) \\ &= \int_0^\infty F_{i'}^{(s)}(z - m^{(d)} - y) f_{i'}(y)\, dy, \end{aligned}$$

where the integral is taken over the support of $\tau_{i',\sigma(i')}$. We use the independence of $\widetilde{t}_{i'}^{(s)}$ and $\tau_{i',\sigma(i')}$, which holds since $\widetilde{t}_{i'}^{(s)}$ depends only on charging durations of predecessors of i' that are independent of $\tau_{i',\sigma(i')}$ by assumption. Combining these results yields the desired formula. ∎

The recursive formula above enables sequential computation of distributions along predecessor chains through nested recursion. For practical evaluation and theoretical analysis, an explicit closed-form integral representation is preferable.

The following theorem provides such a characterization by unrolling the recursion along the entire predecessor chain.

Theorem 1: Consider EV $i_k \in [n]$ with predecessor chain $i_{k-1}, i_{k-2}, \dots, i_{k-l}$ on charger $\sigma(i_k)$, where $pred(i_{k-l}) = 0$ and $pred(i_{k-h}) = i_{k-h-1}$ for $h = 0, 1, \dots, l-1$. Then for any $z \in \mathbb{R}_{>0}$:

$$F^{(s)}_{i_k}(z) = \mathbb{I}\{t^{(s)}_{i_k} \le z\} \int_{\mathbb{R}^l_{>0}} \prod_{\ell=1}^{l} \Big(\mathbb{I}\{t^{(s)}_{i_{k-\ell}} \le \alpha_\ell(z, \mathbf{y})\} \times f_{i_{k-\ell}}(y_{k-\ell+1})\Big)\, d\mathbf{y},$$

where $\mathbf{y} = (y_k, y_{k-1}, \dots, y_{k-l+1})$.

Proof. We proceed by iterative substitution in the recursive formula from Proposition 1. Since $pred(i_k) = i_{k-1} \neq 0$:

$$F^{(s)}_{i_k}(z) = \mathbb{I}\{t^{(s)}_{i_k} \le z\} \int_0^\infty F^{(s)}_{i_{k-1}}(z - m^{(d)} - y_k) f_{i_{k-1}}(y_k)\, dy_k.$$

Applying the recursion to i_{k-1} with $pred(i_{k-1}) = i_{k-2}$:

$$\begin{aligned} F^{(s)}_{i_{k-1}}(z - m^{(d)} - y_k) &= \mathbb{I}\{t^{(s)}_{i_{k-1}} \le z - m^{(d)} - y_k\} \\ &\quad \times \int_0^\infty F^{(s)}_{i_{k-2}}(z - 2m^{(d)} - y_k - y_{k-1}) \\ &\quad \times f_{i_{k-2}}(y_{k-1})\, dy_{k-1}. \end{aligned}$$

Substituting yields:

$$\begin{aligned} F^{(s)}_{i_k}(z) = \mathbb{I}\{t^{(s)}_{i_k} \le z\} &\int_0^\infty \int_0^\infty \\ &\times\; F^{(s)}_{i_{k-2}}(z - 2m^{(d)} - y_k - y_{k-1}) \\ &\times \mathbb{I}\{t^{(s)}_{i_{k-1}} \le z - m^{(d)} - y_k\} f_{i_{k-1}}(y_k) f_{i_{k-2}}(y_{k-1}) \\ &\times dy_k\, dy_{k-1}. \end{aligned}$$

Continuing this process, after h substitutions ($h \le l$):

$$\begin{aligned} F^{(s)}_{i_k}(z) = \mathbb{I}\{t^{(s)}_{i_k} \le z\} &\underbrace{\int_0^\infty \cdots \int_0^\infty}_{h \text{ times}} F^{(s)}_{i_{k-h}}(\alpha_h(z, \mathbf{y})) \\ &\times \prod_{\ell=1}^{h-1} \mathbb{I}\{t^{(s)}_{i_{k-\ell}} \le \alpha_\ell(z, \mathbf{y})\} \\ &\times \prod_{\ell=1}^{h} f_{i_{k-\ell}}(y_{k-\ell+1})\, dy_k\, dy_{k-1} \cdots dy_{k-h+1}. \end{aligned}$$

Setting $h = l$ and using $pred(i_{k-l}) = 0$, Proposition 1 gives:

$$F^{(s)}_{i_{k-l}}(\alpha_l(z, \mathbf{y})) = \mathbb{I}\{t^{(s)}_{i_{k-l}} \le \alpha_l(z, \mathbf{y})\}.$$

Substituting this final expression and incorporating the indicator into the product (with $\ell = l$) yields the stated formula. ■

Corollary 1 (Distribution of realized end times): Under the same conditions as Theorem 1, the cumulative distribution function of the realized charging end time for EV i_k is given by:

$$F^{(e)}_{i_k}(z) = \int_{\mathbb{R}^{l+1}_{>0}} H_k(z, \mathbf{y})\, d\mathbf{y},$$

where $\mathbf{y} = (y_{k+1}, y_k, y_{k-1}, \dots, y_{k-l+1})$ and

$$H_k(z, \mathbf{y}) = \prod_{\ell=0}^{l} \Big(\mathbb{I}\{t^{(s)}_{i_{k-\ell}} \le z - \ell \cdot m^{(d)} - \sum_{j=0}^{\ell} y_{k-j+1}\} \cdot f_{i_{k-\ell}}(y_{k-\ell+1})\Big).$$

Proof. By definition, $\widetilde{t}^{(e)}_{i_k} = \widetilde{t}^{(s)}_{i_k} + \tau_{i_k,\sigma(i_k)}$. Therefore:

$$F^{(e)}_{i_k}(z) = \mathbb{P}\left(\widetilde{t}^{(s)}_{i_k} + \tau_{i_k,\sigma(i_k)} \le z\right).$$

Applying the law of total probability by conditioning on $\tau_{i_k,\sigma(i_k)} = y_{k+1}$:

$$F^{(e)}_{i_k}(z) = \int_0^\infty F^{(s)}_{i_k}(z - y_{k+1}) f_{i_k}(y_{k+1})\, dy_{k+1}.$$

The independence of $\widetilde{t}^{(s)}_{i_k}$ and $\tau_{i_k,\sigma(i_k)}$ follows from the fact that $\widetilde{t}^{(s)}_{i_k}$ depends only on the charging durations of EVs $i_{k-1}, i_{k-2}, \dots, i_{k-l}$, which are independent of $\tau_{i_k,\sigma(i_k)}$ by the mutual independence assumption.

Substituting the explicit formula from Theorem 1 with z replaced by $z - y_{k+1}$, we obtain the stated $(l+1)$-fold integral. ■

While Theorem 1 and Corollary 1 characterize the distributions of realized start and end times, deriving a closed-form expression for the expected peak load $\mathbb{E}(\mathbf{P})$ is analytically intractable due to at least two fundamental obstacles. First, $\mathbf{P}$ involves the expectation of a supremum over a continuous set, which makes it hard to find a simple closed-form representation. Second, the maximum is taken over load values at all time points that depend on the same random variables (stochastic charging durations), inducing complex dependencies across the entire horizon that prevent analytical tractability.

In contrast, the expected total tardiness $\mathbb{E}(\mathbf{T})$ admits an explicit analytical expression via linearity of expectation, as demonstrated in the following corollary. For practical optimization, we employ Monte Carlo simulation to approximate both objectives by sampling from the charging duration distributions and obtaining statistically reliable estimates.

Corollary 2 (Expected Total Tardiness): The expected total tardiness is given by

$$\mathbb{E}\left[\sum_{i\in[n]} \max\left(0, \widetilde{t}^{(e)}_i - d_i\right)\right] = \sum_{i\in[n]} \int_{d_i}^{\infty} \left(1 - F^{(e)}_i(z)\right) dz,$$

with $F^{(e)}_i(z)$ given explicitly by Corollary 1.

Proof. The result follows directly by applying linearity of expectation to equation 4, the standard tail probability formula for non-negative random variables, and the explicit distribution of $\widetilde{t}^{(e)}_i$ given by Corollary 1. The details are omitted. ■

V. Methodology

To address the computational complexity of the EVCSP under stochastic charging durations, we employ MOEAs to approximate the Pareto front. We investigate three state-of-the-art metaheuristics: NSGA-II [15], MOPSO [16], and MOGWO [17]. For MOPSO, we adopt the variant proposed by Sierra and Coello Coello [18]. The algorithms maintain a population of candidate solutions and iteratively evolve them through selection, recombination, and diversification mechanisms. Detailed descriptions of the algorithmic frameworks can be found in the original publications.

A. Solution Representation

Each candidate solution (schedule) in the population is encoded as an $n \times 3$ matrix S, where n denotes the number of EVs. The i-th row $S_i = [j, t_i^{(s)}, t_i^{(e)}]$ represents the scheduling decisions for EV i, specifying: (i)

1) the charger assignment $j \in [m]$ to which EV i is allocated,
2) the planned charging start time $t_i^{(s)} \in \mathbb{R}_{>0}$, and
3) the planned charging end time $t_i^{(e)} = t_i^{(s)} + r_{i,j}$, where

$$r_{i,j} = \frac{e_i}{w_j}, \tag{9}$$

corresponds to the nominal charging duration under constant power delivery.

B. Stochastic Insertion Heuristic

The stochastic insertion heuristic is a core building block of our evolutionary approach, serving three key purposes: (i) generating initial feasible solutions for the population, (ii) repairing infeasible solutions produced during crossover, and (iii) implementing the mutation operator.

Given a schedule S, EV i, and charger j, the operator attempts to assign EV i to charger j while maintaining feasibility.

The procedure first identifies all idle time intervals on charger j by sorting existing assignments by their planned start times and extracting gaps between consecutive sessions, accounting for the minimum separation time $m^{(d)}$. A charger with N existing assignments yields $N+1$ availability intervals. The algorithm then iterates through these intervals in order until finding the first one satisfying $t_{\text{end}} - \max(t_{\text{start}}, a_i) \geq r_{i,j}$, ensuring sufficient duration to accommodate EV i's mean charging time after its arrival. A planned start time $t_i^{(s)}$ is sampled uniformly within the selected interval, the planned end time is set as $t_i^{(e)} = t_i^{(s)} + r_{i,j}$, and the schedule is updated. Algorithm 1 formalizes this procedure.

To initialize the population for each evolutionary algorithm, we generate random feasible schedules by processing EVs in a random order, where for each EV i in this randomized sequence, we randomly select a charger $j \in [m]$ and apply Algorithm 1 to assign EV i to charger j.

Algorithm 1 Stochastic Insertion Heuristic

Require: Current schedule S, EV i, Charger j
Ensure: Updated schedule S
Identify EVs assigned to charger j and sort by $t_k^{(s)}$
if no EVs assigned to charger j **then**
  $\mathcal{A} \leftarrow \{[0, +\infty)\}$
else
  Let N = number of EVs assigned to charger j
  Construct availability set $\mathcal{A}$ with $N+1$ idle intervals:
    $[0, t_1^{(s)} - m^{(d)}]$
    $[t_k^{(e)} + m^{(d)}, t_{k+1}^{(s)} - m^{(d)}]$ for $k = 1, \dots, N-1$
    $[t_N^{(e)} + m^{(d)}, +\infty)$
end if
for each interval $[t_{\text{start}}, t_{\text{end}}] \in \mathcal{A}$ **do**
  if $t_{\text{end}} - \max(t_{\text{start}}, a_i) \geq r_{i,j}$ **then**
    break {Valid interval found}
  end if
end for
if $t_{\text{end}} < +\infty$ **then**
  Sample $t_i^{(s)} \sim \text{Uniform}(\max(t_{\text{start}}, a_i), t_{\text{end}} - r_{i,j})$
else
  $t_i^{(s)} \leftarrow \max(t_{\text{start}}, a_i) + |\mathcal{N}(0,1)|$
end if
Set $t_i^{(e)} \leftarrow t_i^{(s)} + r_{i,j}$
Update $S_i \leftarrow [j, t_i^{(s)}, t_i^{(e)}]$
return S

C. Crossover and Mutation Operators

We employ the generalized crossover operator proposed in [3], which constructs offspring schedules by inheriting EV assignments from parent solutions while maintaining feasibility. For MOPSO and MOGWO, which originally employ continuous solution combination mechanisms, we replace these with the discrete crossover operator following the approach demonstrated in [19] for job shop problem. As shown in [3], [19], this adaptation effectively transfers promising schedule components between solutions while preserving feasibility constraints in discrete scheduling environments.

The mutation operator perturbs a schedule by randomly reassigning a subset of EVs to promote search space exploration. Given a schedule S and mutation intensity $mut_{int} \in (0,1)$, each EV is considered sequentially in random order. With probability mut_{int}, a EV is selected for reassignment to a randomly chosen charger via the stochastic insertion heuristic, replacing its previous assignment. Algorithm 2 formalizes this procedure.

VI. Computational Experiments

A. Experimental Setup

We conducted computational experiments on real-world instances derived from the ACN-Data dataset [20]. Following [3], we generated 20 test instances of varying scales: $n \in \{50, 100, 150, 200\}$ EVs with $m = \lceil n/3 \rceil$ chargers, yielding 5 instances per size. For each instance, EV arrival times,

Algorithm 2 Mutation Operator

Require: Current schedule S, Mutation intensity mut_{int}
Ensure: Mutated schedule S'

```
S' ← S
I' ← RandomPermutation([n])
for each EV i ∈ I' do
    if Uniform(0,1) < mut_int then
        Sample charger j uniformly from [m]
        S' ← StochasticInsertion(S', i, j)
    end if
end for
return S'
```

departure times, and requested energies were sampled from the ACN-Data distributions. Charger power ratings were randomly drawn from the set $\{3.3, 7.2, 7.7, 9.6, 11, 11.5, 19.2, 22\}$ kW, representing typical Level 2 chargers. All chargers become available at time $t = 0$. The minimum session separation time was set to $m^{(d)} = 5$ minutes.

For each EV-charger pair (i, j), the stochastic charging duration $\tau_{i,j}$ follows a lognormal distribution with mean $r_{i,j} = e_i/w_j$ and standard deviation $0.1r_{i,j}$, yielding a coefficient of variation of 0.1. For a lognormal random variable X with mean $\mathbb{E}[X]$ and standard deviation $\sqrt{\text{Var}(X)}$, the distribution parameters are given by

$$\sigma = \sqrt{\ln\left(1 + \frac{\text{Var}(X)}{\mathbb{E}[X]^2}\right)}, \quad \mu = \ln(\mathbb{E}[X]) - \frac{\sigma^2}{2}.$$

Applying these formulas with $\mathbb{E}[\tau_{i,j}] = r_{i,j}$ and $\sqrt{\text{Var}(\tau_{i,j})} = 0.1r_{i,j}$, the corresponding lognormal parameters for each EV-charger pair are

$$\sigma_{i,j} \approx 0.0998, \quad \mu_{i,j} \approx \ln(r_{i,j}) - 0.005.$$

These parameters ensure that the expected charging duration matches the nominal duration under deterministic conditions while introducing realistic stochastic variability.

All algorithms were implemented in Python 3.8 with Numba JIT compilation for computational efficiency[1], and experiments were conducted on a computer featuring an Intel® Core™ i5-8350U CPU running at 1.70 GHz (with a turbo boost of up to 1.90 GHz) and equipped with 8.00 GB of RAM.

B. Parameter Tuning

Algorithm parameters were tuned via grid search to ensure fair comparison across all methods. The parameter space was systematically explored over multiple candidate values for each tunable parameter, as reported in Table I. For each algorithm and instance, we evaluated all combinations of candidate parameter values over $n_{\text{trials}} = 5$ independent replications and selected the configuration achieving the best mean hypervolume.

[1]https://github.com/aikhiar/EVCSPStochasticChargingDurationsV2

TABLE I: Parameter ranges for grid search tuning

Parameter	**Candidate Values**
Mutation intensity mut_{int}	{0.01, 0.03, 0.05, 0.07}
Mutation rate	{0.05, 0.10, 0.15, 0.20}
Archive grid divisions (MOPSO, MOGWO)	{10, 12, 15}
Population size N_{pop}	80 (fixed)
Generations L	200 (fixed)
Archive size (MOPSO, MOGWO)	100 (fixed)
Variance factor	0.1 (fixed)
Monte Carlo replications	25 (fixed)

C. Results Discussion

To assess the comparative performance of NSGA-II, MOPSO, and MOGWO, we employ the hypervolume indicator [21], which quantifies the volume of objective space dominated by a Pareto front approximation relative to a reference point. Each algorithm was executed 30 independent times on every instance, using 25 Monte Carlo replications for objective function approximation. This sample size balances estimation accuracy with computational efficiency: given the moderate variance from lognormal charging durations and the large number of fitness evaluations required by each algorithm (16,000 per run), 25 replications provide sufficiently stable estimates while maintaining reasonable computational cost. Table II reports the mean hypervolume values with standard deviations in parentheses.

TABLE II: Mean hypervolume per instance (30 runs)

Instance	**NSGA-II**	**MOPSO**	**MOGWO**
Instance 1 ($n = 50$)	0.582 (0.096)	**0.590 (0.153)**	0.496 (0.122)
Instance 2 ($n = 50$)	0.678 (0.090)	**0.796 (0.052)**	0.571 (0.161)
Instance 3 ($n = 50$)	**0.690 (0.118)**	0.675 (0.091)	0.678 (0.136)
Instance 4 ($n = 50$)	**0.377 (0.140)**	0.334 (0.234)	0.177 (0.212)
Instance 5 ($n = 50$)	**0.465 (0.151)**	0.230 (0.182)	0.177 (0.165)
Instance 6 ($n = 100$)	**0.341 (0.158)**	0.152 (0.144)	0.142 (0.160)
Instance 7 ($n = 100$)	**0.633 (0.131)**	0.449 (0.183)	0.408 (0.169)
Instance 8 ($n = 100$)	**0.603 (0.081)**	0.534 (0.193)	0.460 (0.156)
Instance 9 ($n = 100$)	**0.794 (0.088)**	0.625 (0.143)	0.422 (0.218)
Instance 10 ($n = 100$)	0.577 (0.113)	**0.624 (0.188)**	0.464 (0.169)
Instance 11 ($n = 150$)	**0.616 (0.108)**	0.561 (0.107)	0.554 (0.120)
Instance 12 ($n = 150$)	**0.163 (0.189)**	0.131 (0.206)	0.097 (0.183)
Instance 13 ($n = 150$)	**0.694 (0.049)**	0.610 (0.096)	0.620 (0.088)
Instance 14 ($n = 150$)	**0.753 (0.077)**	0.463 (0.197)	0.314 (0.314)
Instance 15 ($n = 150$)	0.418 (0.144)	**0.621 (0.157)**	0.355 (0.244)
Instance 16 ($n = 200$)	**0.694 (0.111)**	0.314 (0.240)	0.439 (0.226)
Instance 17 ($n = 200$)	**0.790 (0.063)**	0.554 (0.119)	0.567 (0.130)
Instance 18 ($n = 200$)	**0.726 (0.079)**	0.687 (0.096)	0.468 (0.168)
Instance 19 ($n = 200$)	**0.701 (0.080)**	0.623 (0.136)	0.625 (0.099)
Instance 20 ($n = 200$)	0.655 (0.107)	**0.661 (0.153)**	0.401 (0.139)

The results indicate that NSGA-II achieves the highest average hypervolume across all instances (0.598), followed by MOPSO (0.512) and MOGWO (0.422), demonstrating superior convergence and diversity characteristics. NSGA-II achieves the best performance on 15 out of 20 instances, demonstrating consistent superiority across varying problem scales. However, performance exhibits instance-dependent variability, with MOPSO outperforming NSGA-II on 4 instances (Instances 1, 2, 10, and 15), suggesting that problem structure influences relative algorithm effectiveness. Notably, NSGA-II maintains more consistent performance across problem sizes, as evidenced by its lower variability in standard deviations compared to MOPSO and MOGWO.

To illustrate algorithm performance and convergence behavior, we present convergence plots and obtained Pareto fronts for four representative instances: Instance 5 (n=50), Instance 10 (n=100), Instance 15 (n=150), and Instance 20 (n=200) in Figures 1 and 2, respectively. In Figure 1, the solid lines represent mean hypervolume values and the shaded areas indicate 95% confidence intervals computed from the 30 independent executions. MOGWO exhibits the fastest convergence, reaching plateau within 25–50 generations, yet consistently stabilizes at lower hypervolume levels, indicating premature convergence that explains its last-place ranking despite computational efficiency. NSGA-II and MOPSO demonstrate comparable convergence speeds with overlapping confidence intervals, both exhibiting gradual improvement extending beyond generation 100. Figure 2 presents the obtained Pareto front approximations in the bi-objective space. NSGA-II demonstrates clear dominance across all four instances, producing well-distributed solutions with superior coverage spanning broader regions of the trade-off curve. In instances 5, 10, and 15, MOPSO and MOGWO exhibit comparable performance with significant overlap in restricted regions. Instance 20 reveals MOPSO's superiority over MOGWO with better spread. Notably, MOGWO solutions consistently concentrate in the low-tardiness, high-peak-load region, indicating systematic bias toward minimizing expected total tardiness at the expense of peak load reduction and front diversity. This single-objective-oriented behavior explains MOGWO's premature convergence and inability to effectively explore the complete Pareto front.

To determine whether the observed performance differences are statistically significant, we applied the Friedman test to the per-instance mean hypervolume values. Treating each instance as a block and the three algorithms as treatments, we obtained a test statistic of $\chi_F^2 = 22.5$ with 2 degrees of freedom and p-value < 0.001, indicating that at least one algorithm exhibits significantly different performance at the 5% significance level. Table III reports the average ranks from the Friedman test, with NSGA-II achieving the best (lowest) average rank.

TABLE III: Friedman test average ranks

Algorithm	Average Rank
NSGA-II	**1.25**
MOPSO	2.00
MOGWO	2.75

Subsequent pairwise Mann-Whitney U tests confirm that the performance differences are statistically significant across all algorithm pairs, as shown in Table IV. All comparisons yield p-values well below conventional significance thresholds. These results demonstrate that NSGA-II exhibits superior performance in both hypervolume values and consistency across instances, as evidenced by its best Friedman rank.

NSGA-II's elitist selection and explicit diversity preservation via crowding distance prove particularly effective for this problem's discrete combinatorial structure and stochastic fitness landscape, achieving superior Pareto front coverage and consistency across instance scales.

TABLE IV: Mann-Whitney U test pairwise p-values

Comparison	p-value
NSGA-II vs. MOGWO	1.88×10^{-41}
NSGA-II vs. MOPSO	1.26×10^{-10}
MOPSO vs. MOGWO	2.68×10^{-12}

VII. Conclusion

This paper presented a novel bi-objective optimization framework for the EVCSP under stochastic charging durations, minimizing expected peak load and expected total tardiness while explicitly enforcing non-overlapping charging sessions during objective function computation. Our repair mechanism introduces cascading stochastic dependencies where both start and end times of charging sessions become random variables, fundamentally increasing problem complexity and distinguishing our formulation from prior work.

We derived explicit probability distributions for realized charging session start and end times and established an analytical expression for expected total tardiness. However, given the intractability of computing expected peak load exactly and the computational burden of evaluating high-dimensional integrals, we employed Monte Carlo simulation for efficient objective function approximation. We adapted and compared three MOEAs (NSGA-II, MOPSO, and MOGWO) using the hypervolume indicator. Comprehensive experiments on 20 real-world instances from the ACN-Data dataset with up to 200 EVs showed that NSGA-II achieves superior performance, outperforming the other algorithms on 15 of 20 instances with statistically significant differences confirmed by Friedman and Mann-Whitney U tests.

Future research directions include several promising extensions. First, incorporating preemptive charging policies, multi-level chargers, and expanded objectives such as charging costs and energy consumption would enhance practical applicability and enable richer trade-off analyses. Second, since existing stochastic EVCSP literature rarely addresses multiple sources of uncertainty simultaneously, integrated frameworks accounting for concurrent stochastic factors (dynamic EV arrivals, uncertain departure times, and time-varying electricity prices) represent a natural extension. Third, the analytical complexity motivates investigation of machine learning-assisted surrogate models to accelerate fitness evaluation, while exploring hybrid metaheuristics and decomposition-based approaches may yield further algorithmic improvements for large-scale instances. These extensions would advance both the theoretical foundations and practical deployment of stochastic EV charging scheduling systems.

References

[1] International Energy Agency (IEA), "Global EV Outlook 2025," https://www.iea.org/reports/global-ev-outlook-2025, 2025, iEA, Paris. Licence: CC BY 4.0.

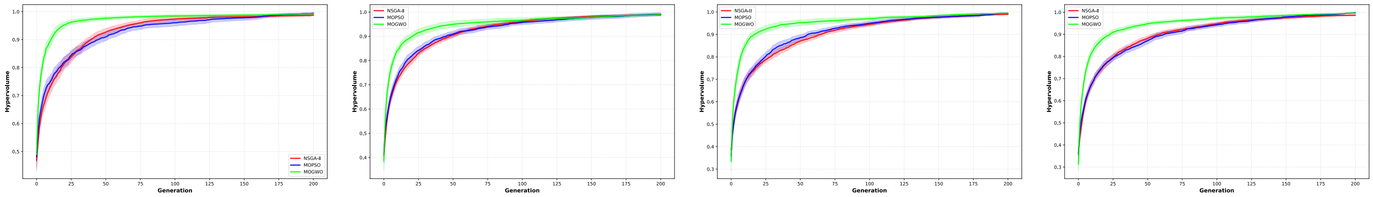

(a) Instance 5 (n=50) (b) Instance 10 (n=100) (c) Instance 15 (n=150) (d) Instance 20 (n=200)

Fig. 1: Convergence plots showing hypervolume evolution over generations for representative instances.

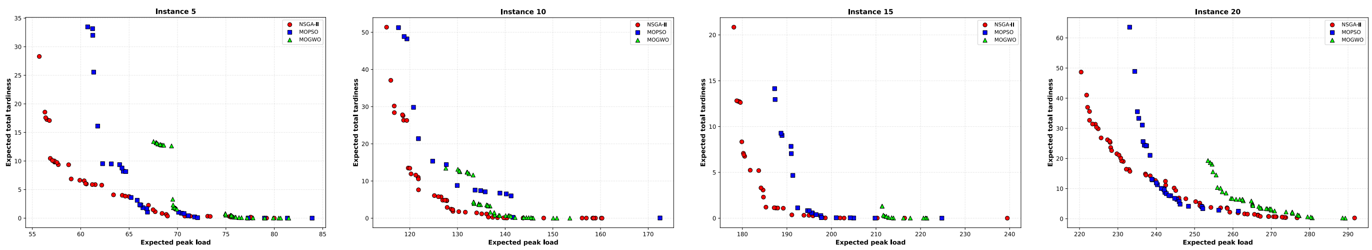

(a) Instance 5 (n=50) (b) Instance 10 (n=100) (c) Instance 15 (n=150) (d) Instance 20 (n=200)

Fig. 2: Obtained Pareto fronts for representative instances.

[2] Z. Lu, T. Xing, and Y. Li, "Optimization of electric bus vehicle scheduling and charging strategies under time-of-use electricity price," *Transportation Research Part E: Logistics and Transportation Review*, vol. 196, p. 104021, 2025. [Online]. Available: https://www.sciencedirect.com/science/article/pii/S1366554525000626

[3] A. Khiar, M. E. A. Brahmia, A. Oulamara, and L. Idoumghar, "Multi-objective electric vehicle charging scheduling under stochastic duration uncertainty," *Omega*, vol. 141, p. 103506, 2026.

[4] M. Golabi, A. Azerine, A. Oulamara, and L. Idoumghar, "Learning-driven optimization with integrated multi-model approaches for efficient electric vehicle charging scheduling," in *2025 IEEE Congress on Evolutionary Computation (CEC)*, 2025, pp. 1–4.

[5] I. Zaidi, A. Oulamara, L. Idoumghar, and M. Basset, "Maximizing the number of satisfied charging demands of electric vehicles on identical chargers," *Omega*, vol. 127, p. 103106, 2024.

[6] A. Azerine, M. Golabi, A. Oulamara, and L. Idoumghar, "A multi-station electric vehicle charging scheduling problem with non-identical chargers," in *2025 IEEE Congress on Evolutionary Computation (CEC)*, 2025, pp. 1–8.

[7] A. Khiar, M. E. A. Brahmia, A. Oulamara, and L. Idoumghar, "Optimized scheduling for electric vehicle charging: A multi-objective approach to grid stability and user satisfaction," in *Proceedings of the 14th International Conference on Operations Research and Enterprise Systems - Volume 1: ICORES*, INSTICC. SciTePress, 2025, pp. 146–155.

[8] I. Zaidi, A. Oulamara, L. Idoumghar, and M. Basset, "Minimizing grid capacity in preemptive electric vehicle charging orchestration: Complexity, exact and heuristic approaches," *European Journal of Operational Research*, vol. 312, no. 1, pp. 22–37, 2024.

[9] R. Chemudupaty, R. Bahmani, G. Fridgen, H. Marxen, and I. Pavić, "Uncertain electric vehicle charging flexibility, its value on spot markets, and the impact of user behaviour," *Applied Energy*, vol. 394, p. 126063, 2025.

[10] B. D. Emami, Y. Zhang, A. Khani, and Y. Song, "Towards an efficient electric bus system: Multi-phase optimization model for incremental electrification of bus network with uncertain energy consumption," *Transportation Research Part C: Emerging Technologies*, vol. 173, p. 105011, Apr. 2025.

[11] A. Khiar, M. E. A. Brahmia, and L. Idoumghar, "Bi-objective electric vehicle charging scheduling with stochastic vehicle arrivals," in *Proceedings of the 15th International Conference on Operations Research and Enterprise Systems - Volume 1: ICORES*, INSTICC. SciTePress, 2026, pp. 65–75.

[12] Y. Gao, L. Yang, M. Wang, and L. Zhen, "Integrated energy scheduling under uncertainty for sustainable ports," *Transportation Research Part E: Logistics and Transportation Review*, vol. 197, p. 104033, May 2025.

[13] Z. Wang, P. Jochem, and W. Fichtner, "A scenario-based stochastic optimization model for charging scheduling of electric vehicles under uncertainties of vehicle availability and charging demand," *Journal of Cleaner Production*, vol. 254, p. 119886, May 2020.

[14] J. James and J. E.A., "Stochastic modeling of electric vehicle charging and impacts on the grid," *Electric Power Systems Research*, vol. 246, p. 111659, 2025.

[15] K. Deb, A. Pratap, S. Agarwal, and T. Meyarivan, "A fast and elitist multiobjective genetic algorithm: Nsga-ii," *IEEE Transactions on Evolutionary Computation*, vol. 6, no. 2, pp. 182–197, 2002.

[16] C. Coello, G. Pulido, and M. Lechuga, "Handling multiple objectives with particle swarm optimization," *IEEE Transactions on Evolutionary Computation*, vol. 8, no. 3, pp. 256–279, 2004.

[17] S. Mirjalili, S. Saremi, S. M. Mirjalili, and L. dos S. Coelho, "Multi-objective grey wolf optimizer: A novel algorithm for multi-criterion optimization," *Expert Systems with Applications*, vol. 47, pp. 106–119, 2016.

[18] M. R. Sierra and C. A. C. Coello, "Improving pso-based multi-objective optimization using crowding, mutation and ε-dominance," in *Evolutionary Multi-Criterion Optimization*, C. A. C. Coello, A. H. Aguirre, and E. Zitzler, Eds. Berlin, Heidelberg: Springer Berlin Heidelberg, 2005, pp. 505–519.

[19] T. Jiang and C. Zhang, "Application of grey wolf optimization for solving combinatorial problems: Job shop and flexible job shop scheduling cases," *IEEE Access*, vol. 6, pp. 26 231–26 240, 2018.

[20] Z. J. Lee, T. Li, and S. H. Low, "ACN-Data: Analysis and applications of an open EV charging dataset," in *Proceedings of the Tenth International Conference on Future Energy Systems*, ser. e-Energy '19, Phoenix, Arizona, jun 2019.

[21] E. Zitzler and L. Thiele, "Multiobjective optimization using evolutionary algorithms — a comparative case study," in *Parallel Problem Solving from Nature — PPSN V*, A. E. Eiben, T. Bäck, M. Schoenauer, and H.-P. Schwefel, Eds. Berlin, Heidelberg: Springer Berlin Heidelberg, 1998, pp. 292–301.